1-9-2006

Electronic structure and vibrational spectra of C_2B_{10}-based clusters and films

Kyungwha Park
Georgetown University, kyungwha@vt.edu

M. R. Pederson
Naval Research Laboratory, Washington D.C.

L. L. Boyer
Naval Research Laboratory, Washington D.C., boyer@dave.nrl.navy.mil

Wai-Ning Mei
University of Nebraska at Omaha, physmei@unomaha.edu

Renat F. Sabirianov
University of Nebraska at Omaha, rsabirianov@mail.unomaha.edu

See next page for additional authors

Electronic structure and vibrational spectra of C_2B_{10}-based clusters and films

Kyungwha Park,[1,2,*] M. R. Pederson,[1] and L. L. Boyer[1,†]
[1]*Center for Computational Materials Science, Naval Research Laboratory, Washington D.C. 20375-5345, USA*
[2]*Department of Physics, Georgetown University, Laboratory, Washington D.C. 20007, USA*

W. N. Mei[3] and R. F. Sabirianov[3]
[3]*Department of Physics, University of Nebraska at Omaha, Omaha, Nebraska 68182, USA*

X. C. Zeng[4] and S. Bulusu[4]
[4]*Department of Chemistry, University of Nebraska at Lincoln, Lincoln, Nebraska 68588, USA*

Seamus Curran[5] and James Dewald[5]
[5]*Department of Physics, New Mexico State University Las Cruces, New Mexico 88003, USA*

Ellen Day[6]
[6]*Department of Mechanical Engineering, University of Nebraska at Lincoln, Lincoln, Nebraska 68588, USA*

Shireen Adenwalla,[7] Manuel Diaz,[7] Luis G. Rosa,[7] S. Balaz,[7] and P. A. Dowben[7]
[7]*Department of Physics, University of Nebraska at Lincoln, Lincoln, Nebraska 68588, USA*
(Received 15 July 2005; revised manuscript received 2 November 2005; published 9 January 2006)

The electronic structure, total energy, and vibrational properties of $C_2B_{10}H_{12}$ (carborane) molecules and C_2B_{10} clusters formed when the hydrogen atoms are removed from carborane molecules are studied using density functional methods and a semiempirical model. Computed vibrational spectra for carborane molecules are shown to be in close agreement with previously published measured spectra taken on carborane solids. Semiconducting boron carbide films are prepared by removing hydrogen from the three polytypes of $C_2B_{10}H_{12}$ deposited on various surfaces. Results from x-ray and Raman scattering measurements on these films are reported. Eleven vibrationally stable structures for C_2B_{10} clusters are described and their energies and highest occupied and lowest unoccupied molecular orbital gaps tabulated. Calculated Raman and infrared spectra are reported for the six lowest-energy clusters. Good agreement with the experimental Raman spectra is achieved from theoretical spectra computed using a Boltzmann distribution of the six lowest-energy free clusters. The agreement is further improved if the computed frequencies are scaled by a factor of 0.94, a descrepancy which could easily arise from comparing results of two different systems: zero-temperature free clusters and room-temperature films. Calculated energies for removal of hydrogen pairs from carborane molecules are reported.

DOI: 10.1103/PhysRevB.73.035109 PACS number(s): 78.30.−j, 31.15.Ew, 36.40.Qv, 81.05.Hd

I. INTRODUCTION

In recent years, films of $C_2B_{10}H_\epsilon$, where $0 \leqslant \epsilon \lesssim 0.8$, have received considerable attention because of their interesting and useful semiconducting properties: adjustable band gap[1] and multiple polytypes.[2] In addition, boron has a high cross section for neutron capture, so small devices can be built out of boron carbide films to detect neutrons and convert the energy of the associated nuclear reactions directly into electrical current. The specific properties of the films, such as band gap[1] and type (*n* or *p*) of conductivity,[3] may vary (or be tuned) by adjusting details of the preparation method. So far, many advances have been made in building a variety of devices, without much theoretical understanding. The difficulty stems from a lack of knowledge about the underlying crystal structure.

The raw materials for making $C_2B_{10}H_\epsilon$ semiconducting films can be any of the three polytypes of dicarba-closo-dodecaboranes, $C_2B_{10}H_{12}$, or simply carboranes. The three polytypes, *para*-, *ortho*-, or *meta*-carborane, have icosahedral-like structures, in which there are three possibilities to place two carbons at the corners of the icosahedron. If the two carbon atoms are located at the opposite corners (or at third-nearest-neighboring corners), they form a *para*-carborane. On the other hand, if the two carbon atoms are

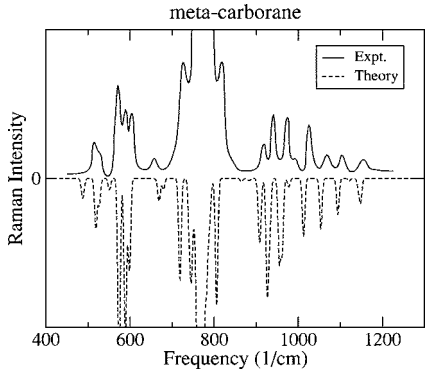

FIG. 1. Comparison of DFT-calculated Raman spectra for the *meta*-carborane molecule with corresponding experimental results for the room-temperature solid (Ref. 7).

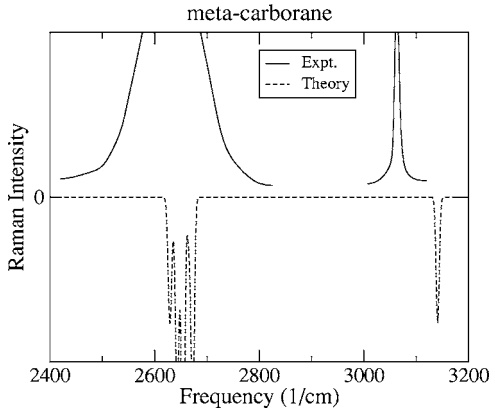

FIG. 2. Comparison of DFT-calculated Raman spectra for the *meta*-carborane molecule with corresponding experimental results for the room-temperature solid (Ref. 7).

placed at second- (first-) nearest-neighboring corners, they form a *meta*- (*ortho*-) carborane.

Semiconducting films form by removing hydrogen from already formed films of $C_2B_{10}H_{12}$ deposited on various surfaces. The hydrogen is removed either by ultraviolet radiation or electron bombardment to produce the desired semiconducting $C_2B_{10}H_\epsilon$ film. Or qualitatively similar films can be obtained by removing hydrogen from $C_2B_{10}H_{12}$ molecules in the gas phase using high-power radio-frequency fields and allowing the resultant clusters to deposit on a suitable substrate.[4,5] The properties of the films formed by these varying techniques are qualitatively similar to each other as long as the value of ϵ is small, $\lesssim 0.8$.

In principle, the structure of the films may not have much in common with the structures of C_2B_{10} clusters. On the other hand, the above facts suggest that some of the properties of the clusters may be retained in the film. In any case, we are motivated to study the properties of C_2B_{10} clusters because (a) their structures may be directly related to structures in the films and (b) our results may be used to characterize the accuracy of energies and forces obtained from more efficient semi empirical simulation methods. This may allow one to ultimately answer structure related questions.

In this paper we first give a brief description of the computational methods used. Then we show that results derived

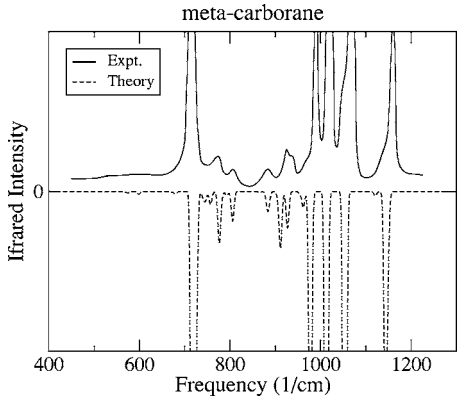

FIG. 3. Comparison of DFT-calculated infrared spectra for the *meta*-carborane molecule with corresponding experimental results for the room-temperature solid (Ref. 7).

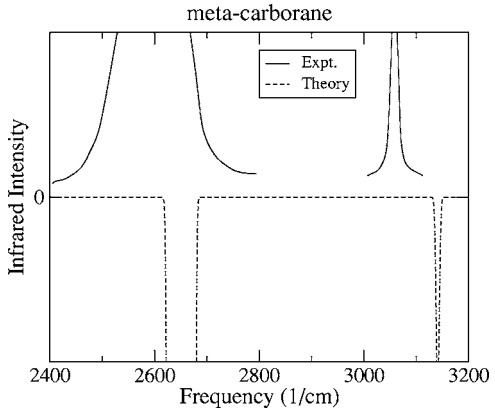

FIG. 4. Comparison of DFT-calculated infrared spectra for the *meta*-carborane molecule with corresponding experimental results for the room-temperature solid (Ref. 7).

from density functional theory[6] (DFT) for the vibrational spectra of carborane molecules correlate closely with measured spectra[7] on solid samples of carborane molecules. Next we report results of Raman spectra and X-ray diffraction measurements on films of $C_2B_{10}H_\epsilon$. This is followed by a detailed description of calculations carried out for free clusters of C_2B_{10}. Eleven different vibrationally stable clusters are identified, and their energies and highest occupied and lowest unoccupied molecular orbital (HOMO-LUMO) gaps reported. Predicted Raman and infrared scattering intensities for the lower-energy structures are reported and compared with experimental Raman data aquired from measurements on films. Finally, results obtained for $C_2B_{10}H_{10}$ clusters are presented and relative energies obtained using DFT and a well-known semiempirical model are compared.

II. COMPUTATIONAL METHODS

The total energy and forces exerted on all atoms are calculated using a DFT code NRLMOL,[8–14] in which all electrons are taken into account with Gaussian basis sets within the generalized gradient approximation[15] (GGA). The forces are

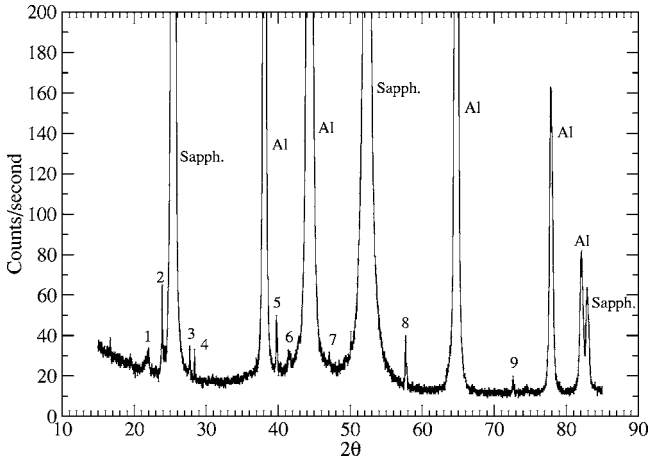

FIG. 5. X-ray diffraction data for a sample on a Al_2O_3 (sapphire) substrate.

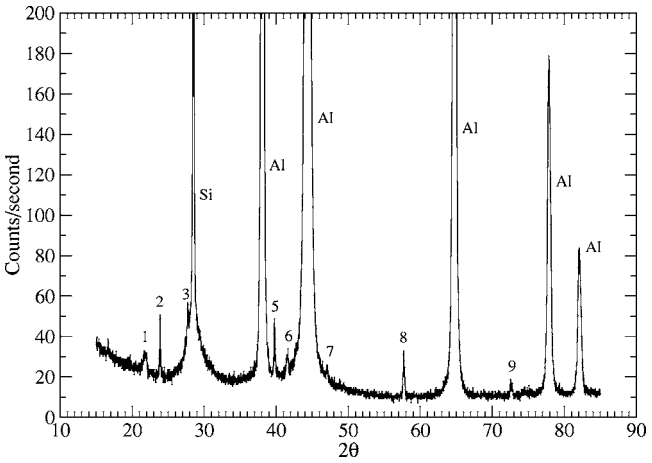

FIG. 6. X-ray diffraction data for a sample on a silicon substrate.

used to determine full structural relaxations and the dynamical matrices from which vibrational frequencies and normal modes are derived.[16] We also use a plane-wave pseudopotential DFT approach combined with Monte Carlo sampling[17,18] and a semiempirical model (PM3-NDO) from the HYPERCHEM package[19] to suggest structures and to compare with the DFT results.

III. ELECTRONIC STRUCTURE AND VIBRATIONAL SPECTRA OF $C_2B_{10}H_{12}$ MOLECULES AND SOLIDS

A possible model for the structure of C_2B_{10} films assumes that the icosahedral-like cage structures of the carborane molecules remain intact when the hydrogen atoms are removed, with neighboring cages replacing the 12 hydrogens. Thus, we are motivated to compute the vibrational spectra of carborane molecules.

Fully relaxed structures for isolated *ortho*-, *meta*-, and *para*-carborane molecules and their vibrational modes have been determined using DFT and NRLMOL. The eigenvalues of the dynamical matrices are all $\geqslant 0$ (zero corresponding to free translation and rotation); i.e., all vibrational modes are stable and the structure is said to be vibrationally stable. The energy levels in the Kohn-Sham method[6] provide an estimate of the energy levels (orbitals) of the molecule. And the difference between the lowest unoccupied molecular orbital and the highest occupied molecular orbital denotes the HOMO-LUMO gap. The DFT-calculated HOMO-LUMO gaps for $C_2B_{10}H_{12}$ are 6.54, 6.75, and 6.86 eV for *ortho*-, *meta*-, and *para*-carborane, respectively. The DFT calculated HOMO-LUMO gaps are typically underesimated, so the above HOMO-LUMO gaps are also likely underestimated. The semiempirical model (PM3-NDO) yeilds HOMO-LUMO gaps of approximately 10 eV for all three types of $C_2B_{10}H_{12}$.[2,20]

Raman and infrared spectra of the carboranes have been

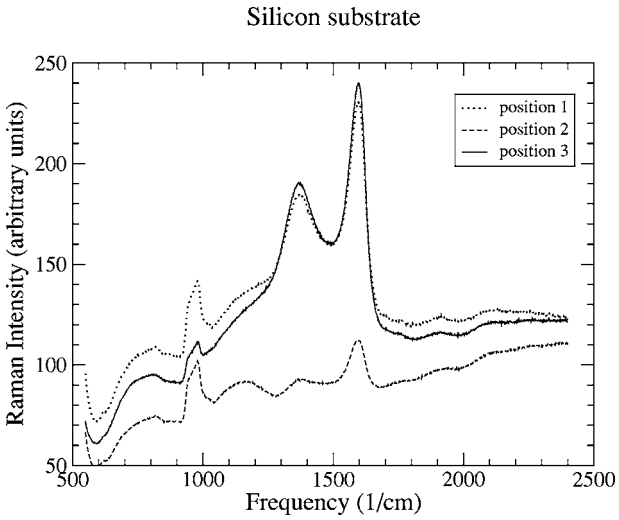

FIG. 7. Raman spectra from three randomly selected positions in the silicon substrate sample.

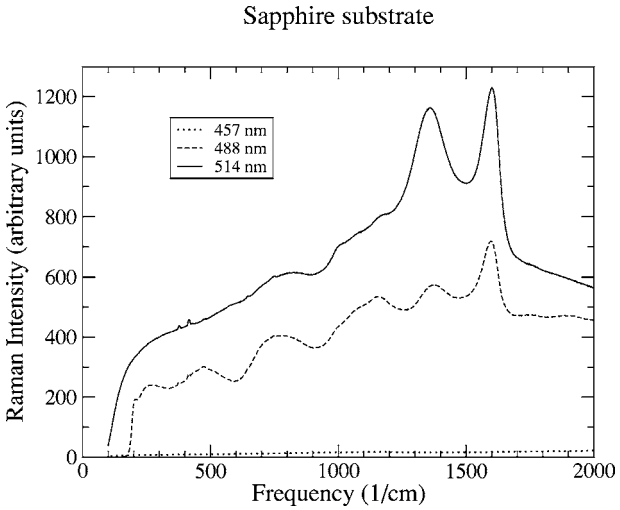

FIG. 8. Raman spectra obtained using three different laser frequencies for the sample with a sapphire substrate.

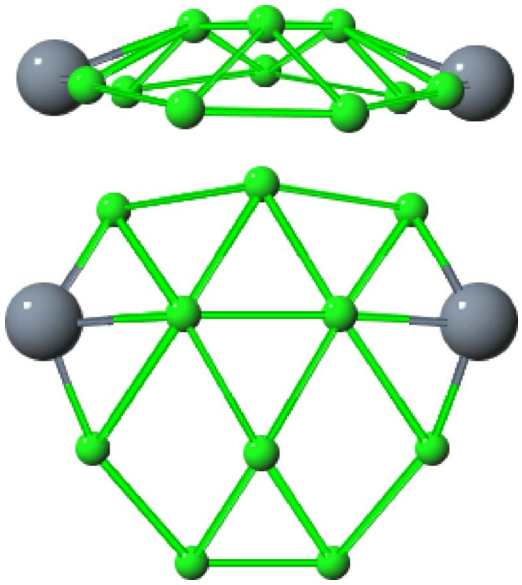

FIG. 9. (Color online) GS structure.

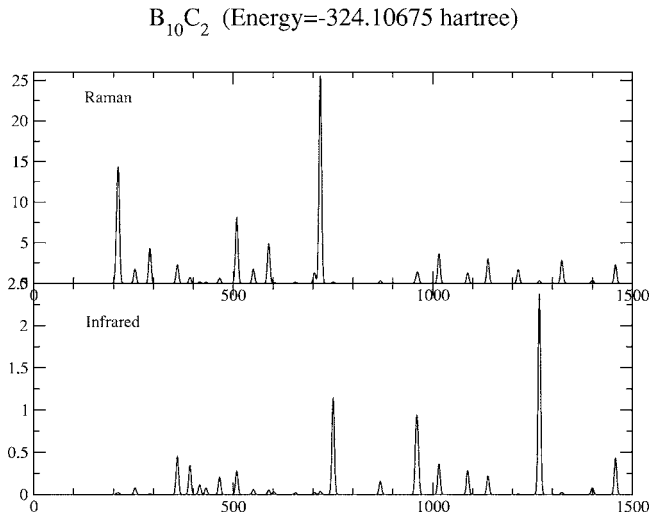

FIG. 10. Vibrational spectrum for the GS structure.

determined using NRLMOL. Calculated vibrational frequencies are considered accurate to within an uncertainty of ~30 cm^{-1}. The infrared absorption and Raman scattering intensities are computed assuming the harmonic approximation with normal-mode levels populated for a temperature of 300 K, random sampling of cluster orientation, and an arbitrary choice for peak width.

Experimentally determined spectra taken from the work of Leites[7] have been digitized to facilitate comparison with our computed spectra. The comparison is illustrated for *meta*-carborane in Figs. 1–4. Specifically, we compare with the data labeled 2 in Fig. 2 of Leites[7] and we plot frequency increasing from left to right.

The comparisons for *ortho*- and *para*-carborane are qualitatively similar to that of *meta*-carborane. There is a gap in the vibrational spectra between 1200 and 2500 cm^{-1} for all three carboranes, with high-frequency modes dominated by motion of the hydrogen atoms.

These results show that (1) the vibrational properties of solids, at least in this case, are very similar to that of the free cluster constituents and (2) the accuracy of DFT as employed in NRLMOL is certainly good enough to identify the carborane clusters from their vibrational spectra.

IV. EXPERIMENTAL X-RAY AND RAMAN SPECTRA FOR $C_2B_{10}H_\epsilon$ FILMS

Thin films of semiconducting boron carbide were deposited via plasma-enhanced chemical vapor deposition using a custom-made parallel-plate radio-frequency reactor. The films were deposited using argon as the carrier gas for the source molecule, which in this case was *ortho*-carborane. A constant pressure of 200 mTorr was maintained throughout the etching and deposition of the substrates and film. Si(111) and Al_2O_3 (012) substrates were chemically cleaned prior to insertion and etched in an Ar plasma for 30 min before film deposition. A constant temperature of 344 C was maintained throughout the entire process. Note that both deposits were made simultaneously: hence any differences in structure or composition are wholly due to the differing growth modes on the two substrates. Using x-ray reflectivity as a calibration for growth thickness the film thickness was estimated to be 600 nm on Al_2O_3 and 1500 nm on silicon. Four samples for each substrate (eight total) were created by the above-described method. Each sample produced results qualitatively similar to those described below.

X-ray diffraction measurements on both films show peaks that correlate with the Al holder and substrates. The additional structure is similar on both films, indicating that the boron carbide films are structurally similar and not significantly dependent on the substrate. These data are tabulated in Table I, with peak positions identified and labeled according to substrate, sample, and holder. The larger-angle peaks for Al do not fall precisely at values obtained by applying Bragg's law to the Al(111) peak. However, comparing these values with numbers obtained from a 0.4%-shifted Al(111) peak (numbers in square brackets) gives us confidence that our aluminum peak assignments are correct.

X-ray diffraction data for samples on sapphire and silicon are plotted in Figs. 5 and 6. We see that all nine peaks identified as coming from the C_2B_{10} sample, with the exception of peak No. 4, are visible in both samples. Peak No. 4 is clearly hidden by the silicon substrate peak (Fig. 6). The sample peaks are all weaker than any that result from the substrate or aluminum holder.

Normalized Raman spectra were obtained using a Renishaw InVia Raman spectrometer equipped with a Raman Leica RE02 microscope. Here 514.7 nm radiation was produced from a 20 mW air-cooled Ar^+ Laser-Physics laser,

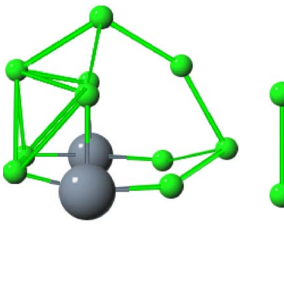

FIG. 11. (Color online) S1 structure.

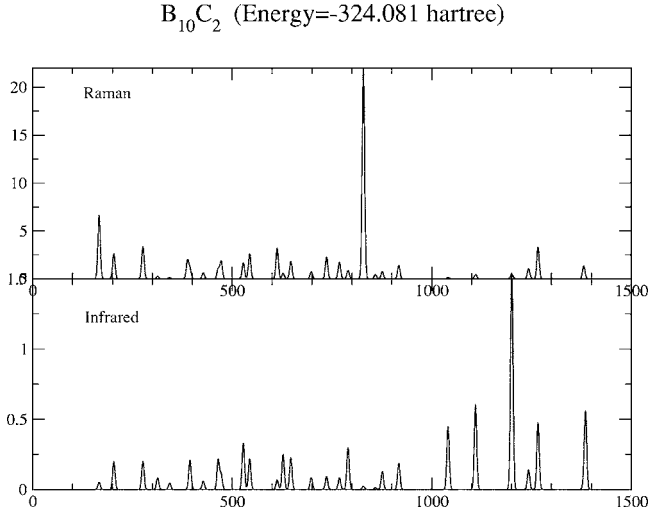

FIG. 12. Vibrational spectrum for the S1 structure.

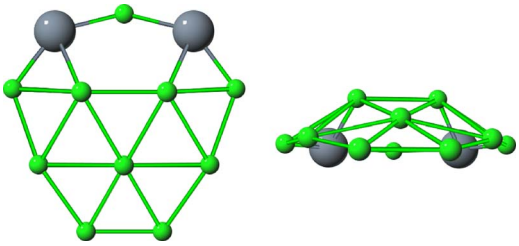

FIG. 13. (Color online) SG1 structure.

operating at laser powers from 1% to 100%. The Raman band of silicon (520 nm) was used to calibrate the spectrometer, with a resolution better than 1.5 cm^{-1}.

Raman spectra of boron carbide deposited on Si and Al_2O_3 are shown in Figs. 7 and 8, respectively. Spectra for the silicon substrate sample were taken using a 488-nm laser at full power. The sample was mounted and scans were taken for 10 s with 10 acquisitions per position. Once the scan was finished, the sample was moved vertically to a second position and the scan repeated. The reproducibility of the peak positions in all three scans is indicative of the spatial homogeneity of the sample.

The spectra for the sample with the Al_2O_3 substrate, shown in Fig. 8, were collected using lasers of varying wavelengths, all set to full power. The exposure time for this sample was 15 s with 30 acqusitions per scan.

The Raman spectra on both samples show two prominent peaks positioned at 1600 cm^{-1} and 1365 cm^{-1} which correspond to two peaks identified by McIllroy *et al.*[21] for CB_4 nanowires. Other less prominent peaks from the boron carbide films occur at ~1150 cm^{-1} and at ~750 cm^{-1} for films on both silicon and sapphire. Our data show sharp structure in the Raman spectra at the well-known Raman frequencies for Si and Al_2O_3, giving us further confidence in the exact positions of structure in our data at higher frequencies. The peak at 950 cm^{-1} in Fig. 7 is believed to be an artifact of the silicon substrate, because it was present also on the background scan of the bare silicon substrate.

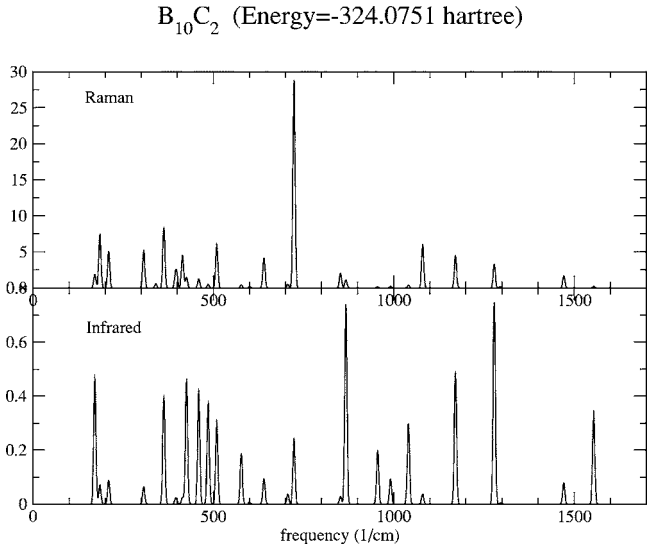

FIG. 14. Vibrational spectrum for the SG1 structure.

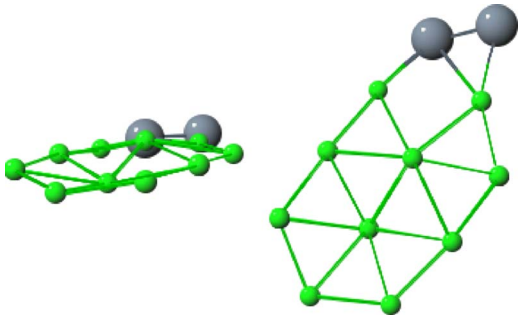

FIG. 15. (Color online) S2 structure

We note that peaks in the experimental Raman spectra extend to 1600 cm^{-1}, well beyond any non-hydrogen-related features in the spectra for $C_2B_{10}H_{12}$ films and clusters (see Sec. III).

V. DFT-CALCULATED ELECTRONIC STRUCTURE AND VIBRATIONAL SPECTRA FOR C_2B_{10} CLUSTERS

As starting geometries for C_2B_{10} clusters, we use the relaxed geometry for $B_{12}H_{12}$, which has the ideal icosahedral symmetry, and relaxed geometries for $C_2B_{10}H_{12}$, which have approximate icosahedral structures. If we start with the $B_{12}H_{12}$ icosahedron, two borons are replaced by two carbons and all hydrogen atoms are removed to construct the geometry for C_2B_{10}. If the two carbon atoms are placed at opposite corners (*para*-carborane), then the number of symmetry operations is reduced from 120 to 20. If the two carbon atoms are placed at first- or second-neighbor positions (*ortho*- or *meta*-carborane), then the number of symmetry operations is reduced to 4.

We first relax the starting geometries for the three different polytypes of C_2B_{10} within the above symmetry constraints using NRLMOL. Each of the relaxed structures is found to have a mildly perturbed icosahedral structure, but they each have two unstable vibrational modes. Hence, we remove the symmetry constraints and carry out further relax-

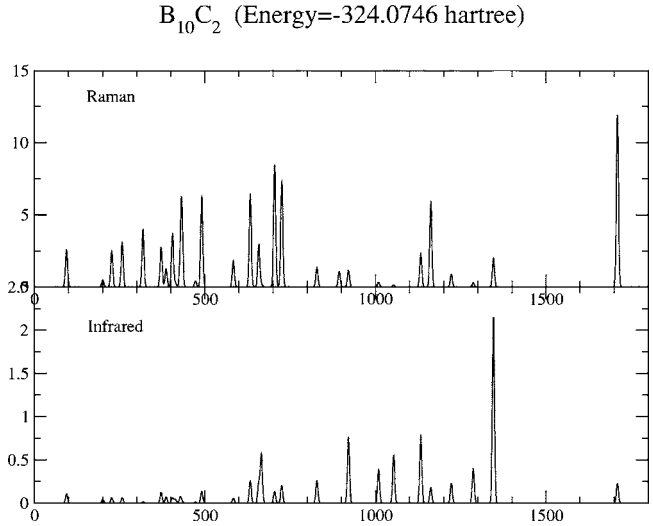

FIG. 16. Vibrational spectrum for the S2 structure.

TABLE I. Positions of x-ray diffraction peaks for samples on $Al_2O_3(012)$ and Si(111) substrates with aluminum holder. Numbers in parentheses are estimated from Braggs law given the measured values for $Al_2O_3(012)$ and Al(111). Numbers in square brackets are similarly based on an assumed value of $2\theta=38.25$ for the Al(111) peak.

2θ Al_2O_3 (deg)	2θ Si (deg)	Identification label
22.0	21.8	1 (sample)
23.92	23.88	2 (sample)
25.48		$Al_2O_3(012)$
27.76	27.72	3 (sample)
28.44		4 (sample)
	28.52	Si(111)
38.10 [38.25]	38.10	Al(111)
39.78	39.78	5 (sample)
41.46	41.58	6 (sample)
44.32 [44.46]	44.30 (44.28)	Al(200)
47.04	47.04	7 (sample)
52.4 (52.34)		$Al_2O_3(024)$
57.70	57.70	8 (sample)
64.68 [64.69]	64.70 (64.42)	Al(220)
72.62	72.62	9 (sample)
77.82 [77.71]	77.84 (77.36)	Al(311)
82.10 [81.88]	82.08 (81.50)	Al(222)
82.90 (82.84)		$Al_2O_3(036)$

ations, starting either from perfect icosahedral positions or from small distortions of the *para, meta*, and *ortho* structures along the calculated unstable normal-mode directions. These relaxations led to four different open-cage or planar structures in which all vibrational modes are stable and all are dramatically different in appearance from the starting icosahedral-like structures. The energies of these clusters are found to be much lower than those of the symmetry-constrained clusters, typically ~3 eV, with atoms moving large distances during the relaxation. We label these clusters S1, S2, S3, and S4 in the order of increasing energy.

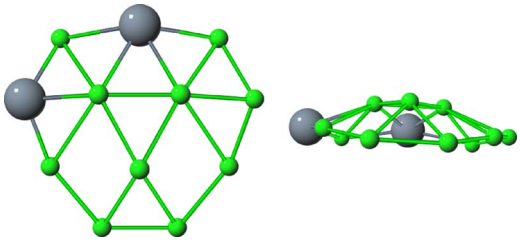

FIG. 17. (Color online) SG2 structure.

The fact that these structures were all derived from icosahedral-like starting geometries suggests that additional stable structures might be produced from a greater variety of starting structures. This possibility was explored using a Monte Carlo technique with a more rapid total energy method,[17,18] and another stable structure was found. It turned out to have an even lower energy than that of S1, as was verified by subsequent calculations using NRLMOL. Since this is the lowest-energy structure determined, we consider it to be a candidate for the ground state (GS) and refer to it as such in subsequent discussion. The calculated ground-state structure shown in Fig. 9 is nearly planar with the two carbon atoms farthest apart. It is similar to the lowest-energy structure $^1A_1$ found in the pure boron cluster B_{12} that has been confirmed by experiment.[22]

The total energies, HOMO-LUMO gaps, and energies per atom relative to the ground state for all structures obtained are listed in Table II. These include structures labeled SG*n* and SE*n* which were obtained, respectively, from interchanging atoms of the ground-state structure and from starting

TABLE II. NRLMOL and GGA total energies, HOMO-LUMO gap energies, and energies relative to that of the ground-state (GS) structure for each of the fourteen structures of C_2B_{10} discussed in the text.

Label	Stability	Structure type	Total Energy (Hartree)	HOMO-LUMO gap (eV)	ΔE (K/atom)
para	unstable	icosahedral cage	−323.890	0.40	5880
ortho	unstable	icosahedral cage	−323.955	0.93	4110
meta	unstable	icosahedral cage	−323.982	0.92	3370
S4	stable	open cage	−324.018	2.18	2390
SE3	stable	cage	−324.023	2.07	2260
SE2	stable	open cage	−324.027	1.75	2150
SG3	stable	planar	−324.034	0.56	1960
S3	stable	open cage	−324.043	2.28	1770
SE1	stable	open cage	−324.068	1.43	1030
SG2	stable	planar	−324.073	1.15	898
S2	stable	planar	−324.0746	1.48	854
SG1	stable	planar	−324.0751	0.40	840
S1	stable	open cage	−324.081	1.97	680
GS	stable	planar	−324.106	1.44	0

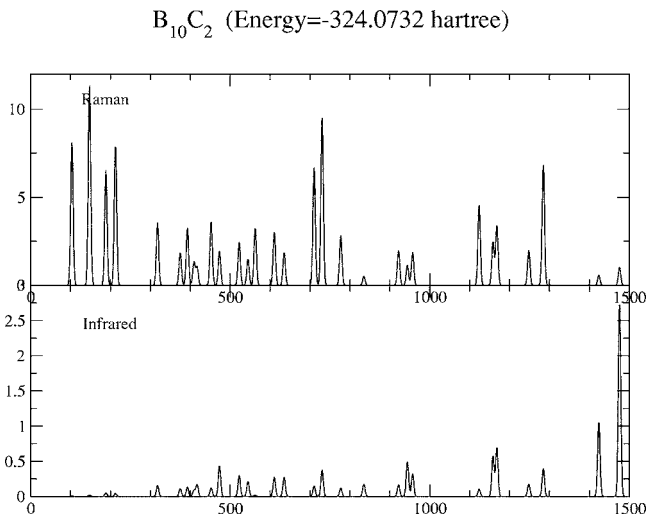

FIG. 18. Vibrational spectrum for the SG2 structure.

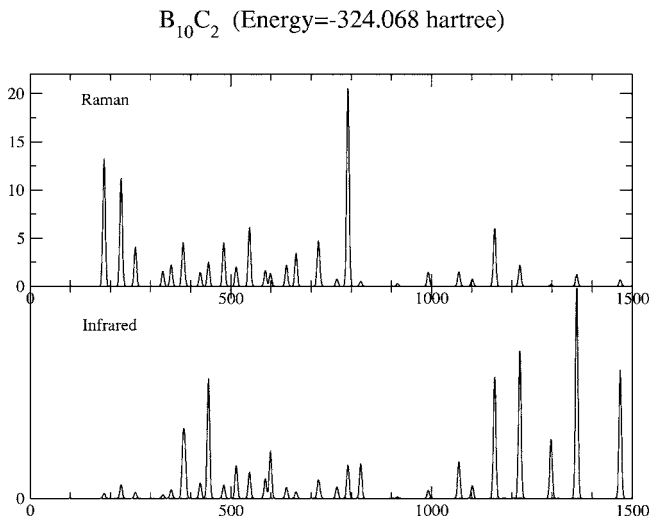

FIG. 20. Vibrational spectrum for the SE1 structure.

structures generated by the empirical model. The HOMO-LUMO gaps are most likely lower bounds, due to the well-known tendency of DFT to underestimate gaps. The accuracy in the energy differences is believed to be within ~10%. Thus, it is likely that the order of energies in Table II is correct, but the reversal of SG1 and S2 is within the expected uncertainty. The structure and vibrational spectra of the six lowest-energy structures are shown in Figs. 9–20. Based on our previous experience with NRLMOL and the GGA we expect computed frequences, shown in wave-number units of cm^{-1}, to be accurate to within ~30 cm^{-1}.

The SG*n* structures were relaxed from the ground-state structure after changing arbitrarily the positions of the two carbon atoms in the ground-state structure. This proceedure led to the three stable structures labeled SG1, SG2, and SG3, of which the lowest-energy one (SG1) has almost the same energy as the S2 structure, despite having a very different structure. Three additional stable structures, labeled SE1, SE2, and SE3, were found by relaxing from geometries derived using the empirical model. The relaxed energies were much lower, as much as 16 eV, than the starting values, indicating the empirical model is not well suited to describe properties of C_2B_{10}. This is further illustrated in Fig. 21 where the structure is depicted for the semiempirical model relaxation and after further relaxation (gaining ~16 eV) using DFT and NRLMOL to form the SE3 structure. We note that SE3 is not very well described as a cage structure, as labeled in Table II. A better description might be small cage with a smaller planer attachment.

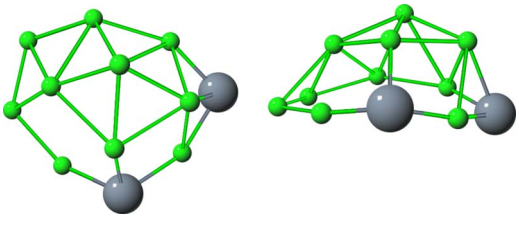

FIG. 19. (Color online) SE1 structure.

VI. RAMAN SPECTRA: COMPARISON WITH CLUSTER CALCULATIONS

The calculated Raman spectra for the GS, SG1, and SG2 structures (Figs. 10, 14, and 18) have their largest peaks around 720 cm^{-1}, while that for the S1 structure has its largest peak around 800 cm^{-1}. Interestingly, the S2 structure has its largest Raman-active peak around 1700 cm^{-1}, which has *not* been found for *any* of the other examined structures. So if the synthesized films are represented by a variety of the (meta)stable clusters, including S2, then a strong peak should appear around 1700 cm^{-1} in measured Raman spectra. Our calculation shows that this peak corresponds mainly to motion of the two carbons in opposite directions along the line between them (see the S2 structure shown in Fig. 15).

The Raman spectra for the sapphire deposited film (Fig. 8, 488-nm curve) is reproduced in Fig. 22 for comparison with our calculated spectra. Panel (b) shows the raw experimental Raman spectrum (thin solid line), a possible Gaussian background (dashed line), and the background-subtracted Raman spectrum (thick solid line). The latter clearly shows a strong peak around 1600 cm^{-1}. We attempt to reproduce the experimental spectrum by assuming that the carborane molecules are effectively heated to very high temperatures, such as 20000 K (≈2 eV), before the hydrogen-depleted fragments deposit onto the substrate. With this assumption we determine a Boltzmann weighting factor for the spectrum of each stable structure to be included in the combined spectrum. Two such combined spectra, and a third using scaled frequencies, are shown in panel (a) of Fig. 22.

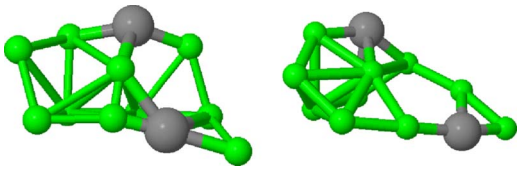

FIG. 21. (Color online) Structure obtained by relaxing from the meta-carborane positions using the empirical model (left) and after further relaxation using DFT and NRLMOL (SE3, right).

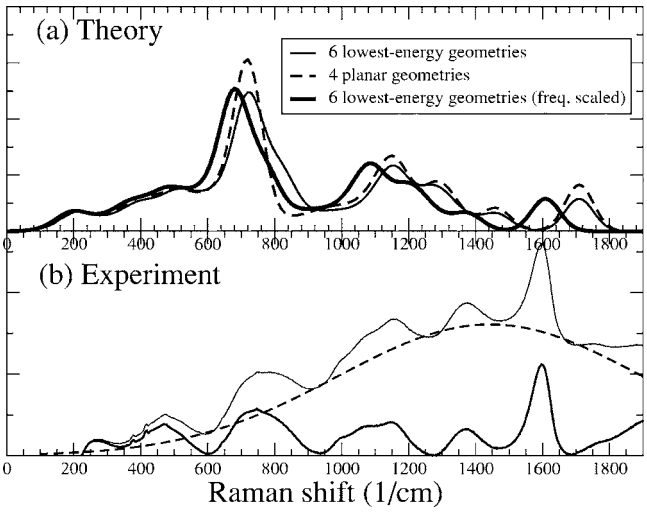

FIG. 22. (a) Computed Raman spectrum for a Boltzmann distribution of the six lowest-energy C_2B_{10} clusters (solid line), those including only the planar structures (dashed line), and the six lowest-energy clusters with frequency scaled by 0.94 (heavy solid line) and (b) experimental data for a $C_2B_{10}H_\epsilon$ film (thin solid line), fitted Gaussian background (dashed line), and data with background removed (thick solid line).

The calculated Boltzmann-weighted spectra are in reasonably good agreement with the experimental spectra, especially if the calculated spectra are scaled by a factor of 0.94 to match the high-frequency peak at 1600 cm^{-1}. A frequency shift of this magnitude is not unexpected from the fact we are comparing spectra derived for zero-temperature free clusters with measured spectra for room-temperature films. The peak at $\sim$700 cm^{-1} in the calculated spectrum is significantly stronger than the corresponding peak in the experimental spectrum. A possible reason may be that the peak at 710 cm^{-1} for the GS structure is highly sensitive to the scattering angle. This is illustrated in Fig. 23.

The calculated spectrum derived from the spectra of planar clusters (GS, SG1, S2, and SG2) agrees with experiment nearly as well as that derived from all six low-energy structures (GS, S1, SG1, S2, SG2, and SE1). This suggests that a reasonable lattice model for the structure of films might be one having layers of triangular boron lattices with random carbon substitutions. On the other hand, including all six structures provides somewhat better agreement in the spectral region near 800 cm^{-1}, suggesting that nonplaner structures are also involved in the structure of the films.

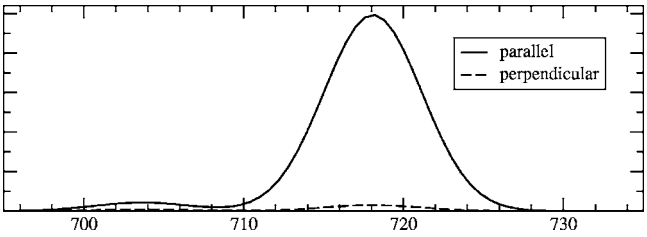

FIG. 23. Raman spectra for the GS structure with parallel and perpendicular scattering angles.

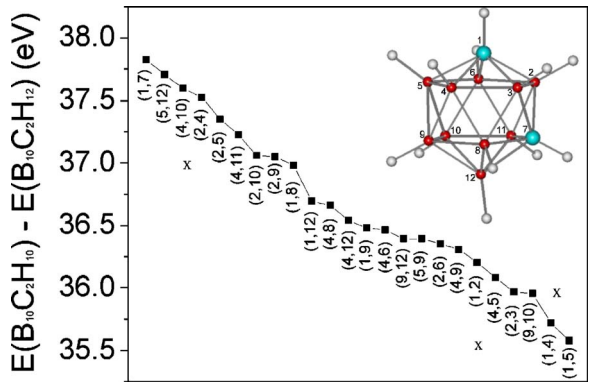

FIG. 24. (Color online) Removal energies for two hydrogens from *meta*-carborane computed using the PM3-NDO semiempirical model. Values marked $\times$ for (4,10), (1,2), and (1,4) were computed using DFT and NRLMOL.

VII. CARBORANE HYDROGEN REMOVAL ENERGIES AND COMPARISON BETWEEN PM3-NDO MODEL AND DFT RESULTS

Thus far we have considered fully hydrogenated carborane molecules and completely dehydrogenated (C_2B_{10}) clusters. In this section we begin to consider the energetics of hydrogen removal from the carborane ($C_2B_{10}H_{12}$) molecules and make some specific comparisons between results using the PM3-NDO semiempirical model and DFT. There are many symmetrically (energetically) different combinations of hydrogen pairs that are candidates for removal—especially so for the *meta*- and *ortho*-carboranes because of their lower-symmetry structures. The possibilities for *meta*-carborane are illustrated in Fig. 24 where the removal energy, as computed by the semiempirical model, is plotted in descending order. Also shown for comparison are three values obtained using DFT. While the $C_2B_{10}H_{10}$ structures remain cage like, within DFT, clearly the relative energies for the semiempirical model are not very reliable.

VIII. CONCLUSIONS

DFT-calculated vibrational spectra for carborane molecules are in excellent agreement with experimental results for solid carborane.

Raman scattering measurements for $C_2B_{10}H_\epsilon$ films show a high-frequency mode near 1600 cm^{-1}, approximately 30% larger than any nonhydrogen modes in carborane films. Based on comparisons with calculated spectra for C_2B_{10} clusters, we tentatively identify this mode with motion of nearest-neighbor carbons in a stable planer-type cluster (S2).

A good overall agreement with experimental Raman data is achieved from a model which combines the spectra of the six lowest-energy C_2B_{10} clusters with 20 000-K Boltzmann weighting factors. In all, we found 11 vibrationally stable C_2B_{10} clusters, and there could well be more. Since most of the low-energy clusters have planer-type structures, we suggest that a possible model for the structure of C_2B_{10} films could be layers of triangular boron lattices with random carbon substitutions.

The semiempirical model (PM3-NDO) from the HYPERCHEM package,[19] known to work reasonably well for the icosahedral-type structures of the carborane molecules, is found to be less reliable for $C_2B_{10}H_{10}$ clusters and very wrong for C_2B_{10} clusters. However, it was useful for generating starting structures for subsequent DFT relaxations.

ACKNOWLEDGMENTS

This work was supported by the U. S. Office of Naval Research (ONR). K.P. was supported by ONR Grant No. N000140211045 and NSF Grant Nos. HRD-0210717 and DMR-0210717.

*Current address: Department of Physics, Virginia Polytechnic Institute and State University, Blacksburg, VA 24061-0435, USA.
†Corresponding author. Electronic address: boyer@dave.nrl.navy.mil

[1] Sunwoo Lee, John Mazurowski, G. Ramseyer, and P. A. Dowben, J. Appl. Phys. **72**, 4925 (1992).
[2] Petru Lunca-Popa, J. I. Brand, Snjezana Balaz, Leuis G Rosa, Mengjun Bai, B. W. Robertson, and P. A. Dowben, J. Phys. D **38**, 1248 (2005).
[3] Anthony N. Caruso, Ravi B. Billa, Snjezana Balaz, Jennifer I. Brand, and P. A. Dowben, J. Phys.: Condens. Matter **16**, L139 (2004).
[4] Dongjin Byun, Seong-don Hwang, P. A. Dowben, F. Keith Perkins, F. Filips, and N. J. Ianno, Appl. Phys. Lett. **64**, 1968 (1994).
[5] Dongjin Byun, B. R. Spady, N. J. Ianno, and P. A. Dowben, Nanostruct. Mater. **5**, 465 (1995).
[6] W. Kohn and L. J. Sham, Phys. Rev. **140**, A1133 (1965).
[7] L. A. Leites, Chem. Rev. (Washington, D.C.) **92**, 279 (1992).
[8] M. R. Pederson and K. A. Jackson, Phys. Rev. B **41**, 7453 (1990).
[9] K. A. Jackson and M. R. Pederson, Phys. Rev. B **42**, 3276 (1990).
[10] M. R. Pederson and K. A. Jackson, Phys. Rev. B **43**, 7312 (1991).
[11] A. A. Quong, M. R. Pederson, and J. L. Feldman, Solid State Commun. **87**, 535 (1993).
[12] D. V. Porezag and M. R. Pederson, Phys. Rev. B **54**, 7830 (1996).
[13] D. V. Porezag, Ph.D. thesis, http://archiv.tu-chemnitz.de/pub/1997/0025
[14] A. Briley, M. R. Pederson, K. A. Jackson, D. C. Patton, and D. V. Porezag, Phys. Rev. B **58**, 1786 (1998).
[15] J. P. Perdew, K. Burke, and M. Ernzerhof, Phys. Rev. Lett. **77**, 3865 (1996).
[16] D. Porezag and M. R. Pederson, Phys. Rev. B **54**, 7830 (1996).
[17] S. Yoo and X. C. Zeng, Angew. Chem., Int. Ed. Engl. **44**, 1491 (2005).
[18] D. J. Wales and H. A. Scheraga, Science **285**, 1368 (1999).
[19] J. J. P. Stewart, J. Comput. Chem. **10**, 209 (1989); **10**, 221 (1989).
[20] A. N. Caruso, L. Bernard, Bo Xu, and P. A. Dowben, J. Phys. Chem. B **107**, 9620 (2003).
[21] D. N. McIllroy, Daqing Zhang, Robert M. Cohen, and J. Wharton, Phys. Rev. B **60**, 4874 (1999).
[22] H. J. Zhai, B. Kiran, J. Li, and L. S. Wang, Nat. Mater. **2**, 827 (2003).